A Neutralizing Antibody Selected from Plasma Cells That Binds to Group 1 and Group 2 Influenza A Hemagglutinins

Davide Corti, *et al.*

Science **333**, 850 (2011);
DOI: 10.1126/science.1205669

35. Details of the data set and analysis can be found in the supporting online material on *Science* Online.
36. In this analysis, residues are considered conserved if they fall within one of the following groups: Asp/Asn/Glu/Gln, Phe/Tyr, Ile/Leu/Val/Met, Lys/Arg, or Ser/Thr.
37. J. L. Lorieau, J. M. Louis, A. Bax, *Proc. Natl. Acad. Sci. U.S.A.* **107**, 11341 (2010).
38. Twenty of the first 23 positions in HA2 are well conserved across all subtypes (fig. S3). Two of the remaining positions (HA2 positions 12 and 15) have differing, group-specific residues. The final position, HA2 residue 19, is also conserved as Asp or Asn across most subtypes from both groups. However, we regard this substitution as nonconservative in the context of CR8020 because $Asp^{19}Asn$ mutations escape virus neutralization.
39. J. Chen, J. J. Skehel, D. C. Wiley, *Proc. Natl. Acad. Sci. U.S.A.* **96**, 8967 (1999).
40. Although there is clear density for the V_L:Arg^{53} side chain placing the guanidinium moiety in close proximity to HA2:Asp^{19}, the preferred rotamer for the Arg side chain cannot be assigned unambiguously. Various rotamers consistent with the observed electron density result in charged atom contact distances of ~4 to 4.5 Å. Although somewhat longer than expected for a salt bridge that would make a major contribution to antibody binding, this discrepancy may be in part due to shielding by a nearby sulfate from the crystallization solution, which is sandwiched between the V_L:Arg^{53}-Arg^{54} side chains.
41. Most of the group 2 HAs with $Asp^{19}Asn$ are restricted to a single, geographically restricted lineage of the H7 subtype, and disproportionate sampling in birds in this region may exaggerate the prevalence of $Asp^{19}Asn$ substitutions in the H7 population (*35*).
42. Neutralization of H15 has not been tested, but the K_d for CR8020 binding is comparable with that of H7, which is neutralized.
43. Neutralization of H14 viruses has not been tested, but comparable binding of CR8020 to H4 and H14 suggests that H14 will not be neutralized.
44. H14 also has a $Glu^{325}Gly$ mutation in HA1, which has a negligible effect on CR8020 binding in a HK68 background.
45. This scenario is reminiscent of the group 1 restriction of CR6261, which cannot interact with group 2 viruses, such as H3 and H7, at least in part due to a conserved glycan at HA1:Asn^{38} and the more general and well-documented use of glycans to mask and unmask surfaces to evade immune recognition, such as vividly illustrated in the evolution of human H1N1 viruses (*12*, *56*).
46. P. A. Bullough, F. M. Hughson, J. J. Skehel, D. C. Wiley, *Nature* **371**, 37 (1994).
47. In contrast, a control mAb against the HA1 head bound to A/Wisconsin/67/2005 HA in all three conformations, and binding was only lost after DTT treatment, which dissociates HA1 from HA2 in the postfusion state.
48. This is evidenced by the fact that, in this case, treatment with DTT did not diminish CR8057 binding to A/Wisconsin/67/2005 HA. In line with its narrow spectrum of neutralization (table S1), CR8057 did not bind to any conformation of the HAs of A/Hong Kong/1/1968 or A/Hong Kong/24/1985.
49. Because the initial crystals only appeared between 3 and 7 days after the start of the experiment, CR8020 must be capable of retaining HA in the prefusion state for several days at low pH.
50. R. Xu, I. A. Wilson, *J. Virol.* **85**, 5172 (2011).
51. G. Russ, K. Poláková, F. Kostolanský, B. Styk, M. Vancíková, *Acta Virol.* **31**, 374 (1987).
52. E. Varecková, V. Mucha, S. A. Wharton, F. Kostolanský, *Arch. Virol.* **148**, 469 (2003).
53. R. Yoshida *et al*., *PLoS Pathog.* **5**, e1000350 (2009).
54. A. M. Hashem *et al*., *Biochem. Biophys. Res. Commun.* **403**, 247 (2010).
55. A. Stropkovská *et al*., *Acta Virol.* **53**, 15 (2009).
56. C. J. Wei *et al*., *Sci. Transl. Med.* **2**, 24ra21 (2010).
57. J. J. Skehel, D. C. Wiley, *Vaccine* **20** (suppl. 2), S51 (2002).

Acknowledgments: We thank H. Tien and D. Marciano of the Robotics Core at the Joint Center for Structural Genomics for automated crystal screening; T. Doukov and the staff of the SSRL BL9-2 for beamline support; X. Dai and R. Stanfield for excellent assistance with data collection, processing, and analyses; R. Lerner, J. Paulson, and D. Burton for valuable comments and insightful discussion; E. Geelen, D. Spek, and V. Klaren for excellent assistance and advice; K. Hegmans, A. Lourbakos, J. Meijer, and A. Apetri and their teams for producing the mAbs and Fabs; C. Y. H. Leung for providing the A/WF/Hong Kong/MPA892/06 virus; E. de Boer-Luijtze and technicians in the groups of P. van Rossum and S. Riemersma for assistance with the animal experiments; E. Brown from Ottawa University, Canada for the mouse-adapted A/Hong Kong/1/68 strain; and A. Dingemans for critical review of the manuscript. This project has been funded in part by the National Institute of Allergy and Infectious Diseases, NIH, Department of Health and Human Services, USA, under contract HHSN272200900060C; the Area of Excellence Scheme of the University Grants Committee, Hong Kong (grant AoE/M-12/06); a predoctoral fellowship from the Achievement Rewards for College Scientists Foundation (D.C.E.); grant GM080209 from the NIH Molecular Evolution Training Program (D.C.E.); and the Skaggs Institute (I.A.W.). Portions of this research were carried out at the Stanford Synchrotron Radiation Lightsource, a national user facility operated by Stanford University on behalf of the U.S. Department of Energy (DOE), Office of Basic Energy Sciences. The Stanford Synchrotron Radiation Lightsource (SSRL) Structural Molecular Biology Program is supported by the DOE Office of Biological and Environmental Research and by NIH, National Center for Research Resources, Biomedical Technology Program, and the National Institute of General Medical Sciences. This is publication 20951 from the Scripps Research Institute. Coordinates and structure factors have been deposited in the Protein Data Bank (PDB code 3SDY). Nucleotide sequences for the CR8020 variable regions have been deposited in GenBank (accession nos. JN093122, JN093123). A patent application relating to antibody CR8020 has been filed (International Publication Number WO2010/130636). Sharing of materials will be subject to standard material transfer agreements.

Supporting Online Material

www.sciencemag.org/cgi/content/full/science.1204839/DC1
Materials and Methods
Figs. S1 to S11
Tables S1 to S7
References

25 February 2011; accepted 10 June 2011
Published online 7 July 2011;
10.1126/science.1204839

A Neutralizing Antibody Selected from Plasma Cells That Binds to Group 1 and Group 2 Influenza A Hemagglutinins

Davide Corti,[1,2]* Jarrod Voss,[3]* Steven J. Gamblin,[3]* Giosiana Codoni,[1]* Annalisa Macagno,[1] David Jarrossay,[1] Sebastien G. Vachieri,[3] Debora Pinna,[1] Andrea Minola,[1] Fabrizia Vanzetta,[2] Chiara Silacci,[1] Blanca M. Fernandez-Rodriguez,[1] Gloria Agatic,[2] Siro Bianchi,[2] Isabella Giacchetto-Sasselli,[1] Lesley Calder,[3] Federica Sallusto,[1] Patrick Collins,[3] Lesley F. Haire,[3] Nigel Temperton,[4] Johannes P. M. Langedijk,[5]† John J. Skehel,[3]‡ Antonio Lanzavecchia[1,6]‡

The isolation of broadly neutralizing antibodies against influenza A viruses has been a long-sought goal for therapeutic approaches and vaccine design. Using a single-cell culture method for screening large numbers of human plasma cells, we isolated a neutralizing monoclonal antibody that recognized the hemagglutinin (HA) glycoprotein of all 16 subtypes and neutralized both group 1 and group 2 influenza A viruses. Passive transfer of this antibody conferred protection to mice and ferrets. Complexes with HAs from the group 1 H1 and the group 2 H3 subtypes analyzed by x-ray crystallography showed that the antibody bound to a conserved epitope in the F subdomain. This antibody may be used for passive protection and to inform vaccine design because of its broad specificity and neutralization potency.

Hemagglutinin (HA) is the main target of influenza A virus–neutralizing antibodies and undergoes continuous evolution driven by the selective pressure of the antibody response, which is primarily directed against the membrane-distal receptor-binding subdomain of the molecule (*1*). Genetically, there are 16 influenza A subtypes of HA, which form two groups (*2*, *3*). Antibodies elicited by vaccination or infection neutralize primarily homologous strains within a given subtype, and new vaccines are produced every year to match these strains (*4*, *5*). Heterosubtypic antibodies capable of neutralizing multiple subtypes within group 1 or group 2 have been isolated from immunized mice, phage libraries, and memory B cells and plasma cells of immune donors (*6*–*11*). In addition, globular head–specific antibodies that cross-react with particular strains of group 1 and group 2 subtypes have been isolated from immunized mice (*12*). However, influenza A–neutralizing antibodies

[1]Institute for Research in Biomedicine, 6500 Bellinzona, Switzerland. [2]Humabs BioMed SA, 6500 Bellinzona, Switzerland. [3]Medical Research Council (MRC) National Institute for Medical Research, The Ridgeway, Mill Hill, London NW7 1AA, UK. [4]Viral Pseudotype Unit, School of Pharmacy, University of Kent, Kent ME4 4TB, UK. [5]Pepscan Therapeutics BV, Lelystad, 8243 RC, Netherlands. [6]Institute of Microbiology, Eidgenössische Technische Hochschule (ETH) Zürich, 8032 Zürich, Switzerland.

*These authors contributed equally to this work.
†Present address: Crucell Holland BV, 2333 CN Leiden, Netherlands.
‡To whom correspondence should be addressed. E-mail: lanzavecchia@irb.unisi.ch (A.L.); skehelj@nimr.mrc.ac.uk (J.J.S.)

targeting epitopes conserved on all 16 subtypes of group 1 and group 2 viruses have not been found so far, and their isolation remains a major goal for therapeutic approaches and vaccine design.

Antibody selection from cultures of single plasma cells. Peripheral blood plasma cells isolated 1 week after vaccination or infection are largely antigen-specific and hence they represent a large repertoire of antibody specificities. Because pan–influenza A–neutralizing antibodies might be extremely rare, we developed a high-throughput culture method to interrogate large numbers of human plasma cells. The method involves culture of single plasma cells in medium supplemented with interleukin-6 (IL-6), a cytokine that supports plasma cell survival (*13*), followed by screening of the culture supernatants with multiple parallel binding assays (*14*) and rescue of the selected antibodies by single-cell reverse transcription polymerase chain reaction (RT-PCR) (*15*). We therefore isolated plasma cells from selected donors who had been previously found to produce a strong heterosubtypic antibody response (*9*), shortly after natural infection with influenza A or vaccination (*16*). Monoclonal antibodies derived from the culture of single plasma cells were tested against the homologous HA, a heterologous group 1 HA (H5, A/Vietnam/1203/04), and a heterologous group 2 HA (H7, A/Netherlands/219/03) (Fig. 1). We interrogated a total of 104,000 plasma cells from eight donors. From one donor, we isolated plasma cells ~1 week after H1N1 swine origin influenza virus (SOIV) infection in November 2009 and 7 days after vaccination with the seasonal vaccine in January 2010. In response to H1N1 SOIV infection, most of the HA-specific plasma cell–derived antibodies (89.7%) bound to SOIV HA (A/Califomia/04/09) and to H5 A/Vietnam/1203/04 HA, which indicated that infection with SOIV boosted a rapid response by cross-reactive memory B cells. Only a few of these antibodies also cross-reacted with H7 HA (such as FI442 and FI510 in Fig. 1A). This donor's response to the seasonal vaccine (containing H1, H3, and influenza B antigens) was largely vaccine-specific (98.2%) (Fig. 1B), consistent with a strong recall response of subtype-specific memory B cells. There were, however, a few antibodies that cross-reacted with H5 HA, and of these, two (FI802 and FI804) cross-reacted also with H7 HA (Fig. 1B). These findings demonstrate that rare antibodies recognizing both group 1 and group 2 HAs can be obtained after natural infection or vaccination.

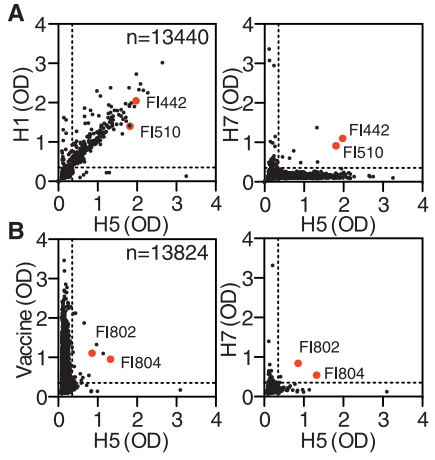

Fig. 1. Identification of monoclonal antibodies binding to group 1 and group 2 HAs in single–plasma cell cultures. Circulating $CD138^+$ cells were isolated from a selected donor ~1 week after infection with SOIV H1N1 (**A**), and 7 days after vaccination (**B**), and cultured at 0.5 cells/well for 4 days. Culture supernatants were tested by ELISA for the presence of IgG antibodies that bound to the homologous recombinant HA molecule (H1 CA/09) or to the seasonal 2009–10 vaccine, and to the heterologous group 1 HA (H5 VN/04) and to the heterologous group 2 HA (H7 NE/03). Each dot represents, for each of the tested antigens, the optical density (OD) values of individual cultures. Plasma cells from selected cultures were harvested, and V_H and V_L gene transcripts were retrieved by single-cell RT-PCR. The red dots indicate cultures that contain IgG reactive against group 1 and group 2 HAs and carrying identical V_H and V_K sequences. Dotted lines indicate background values.

A neutralizing antibody selected in vivo for binding to group 1 and 2 HAs. The sequences of the variable regions of immunoglobulin heavy chain (V_H) and kappa light chain (V_K) retrieved from the four plasma cells producing H1/H5/H7 cross-reactive antibodies were identical. The sequences encoded an antibody that was named FI6 (*17*). FI6 was made up of V_H3-30*18 and V_K4-1*01, had a long heavy chain complementarity-determining region 3 (HCDR3) (22 amino acids), and had a large amount of somatic mutations in both V_H and V_K genes (fig. S1). A clonally related antibody (FI370), carrying the same rearrangements as FI6 on heavy and light chains and some shared somatic mutations, was found among 663 H1/H5-specific plasma cells in the November 2009 experiment (fig. S1).

The FI6 V_H and V_K genes were cloned into expression vectors, and recombinant antibodies were produced by transfecting 293F cells. We also produced the FI6 germline version (FI6-GL), the clonally related FI370 antibody, and an antibody containing all the mutations shared by FI6 and FI370 that represents the evolutionary branching point (FI6/370-BP) (fig. S2A). Purified antibodies were tested for binding and neutralizing activity against multiple HAs and viruses of different subtypes (Fig. 2). FI6 bound all recombinant or purified HAs tested belonging to group 1 (H1, H2, H5, H6, H8, and H9) and group 2 (H3, H4, H7, and H10) with half maximal effective concentration (EC_{50}) values ranging from 10 to 270 ng/ml (Fig. 2A). In addition, FI6 stained cells transfected with HA genes belonging to group 1 (H11, H12, H13, and H16) and group 2 (H4, H10, H14, and H15 (fig. S3). FI6 also neutralized group 1 (H1 and H5) and group 2 (H3 and H7) pseudoviruses and viruses, including the 1918 "Spanish flu" isolate (Fig. 2, B and C). In contrast, FI6-GL and FI370 bound HAs and neutralized viruses of group 1, but not group 2, whereas the FI6/370-BP bound group 1 and, with low efficiency, group 2 HAs (Fig. 2A and fig. S2, B and C). These findings suggest that the FI6-GL was initially selected by a group 1 virus and developed to a branching point characterized by low-level binding to group 2 HA. From this point, the final products FI370 and FI6 may have been selected for binding to group 1 or group 2 HAs, respectively.

The contribution of somatic mutations to FI6 binding to group 2 HAs was further dissected by producing FI6 variant antibodies in which single or multiple mutations in V_H and V_K genes were reverted to the germline (fig. S1). Binding to group 2 HA required somatic mutations present in the CDRs of both V_H and V_K and did not rely on framework mutations (fig. S4). Reversion of single mutations in the CDRs did not lead to a significant loss of binding to group 2 HA, with the exception of the V_K R93S mutant (in which Arg^{93} is replaced by Ser) and the V_K F^{27D}-S mutant (in which Phe^{27D} is replaced by Ser), which led to a decrease in binding by factors of 44 and 12, respectively (fig. S4). On the basis of these findings, we designed an optimized FI6 variant that lacks unnecessary somatic mutations in the framework regions [including the glycosylation site at position 75 in the heavy chain framework region 3 (HFR3)] and two potentially harmful residues, that is, an aspartate isomerization site at position 53–54 of HCDR2 and an acidic cleavage site at position 101–102 of HCDR3 (fig. S1) (*18*). This variant, called FI6v3, showed binding and in vitro neutralizing properties comparable to those of FI6 (Fig. 2 and fig. S4).

The above findings demonstrate the power of the single–plasma cell culture method, which allowed the interrogation of thousands of plasma cells and led to the isolation of a rare pan–influenza A–neutralizing antibody. The rarity of this antibody is underscored by the fact that, from interrogation of plasma cells isolated from seven other donors, we isolated several antibodies that, although they bound to group 1 and group 2 HAs (such as FJ76 in Fig. 2), were unable to neutralize virus infectivity. Notably, the FI6 antibody was not found among ~20,000 immortalized B cell clones generated from memory B cells of the same donor.

Structures of FI6v3-H1 and FI6v3-H3 complexes. The epitope recognized by FI6 was considered likely to be located in the F subdomain of HA, on the basis of the initial finding that FI6 inhibited syncytia formation but not hemagglutination (fig. S5), bound near the HA membrane anchor in electron microscopy images of FI6-HA complexes (fig. S6), and competed for binding to HAs with the previously described group 1–specific antibody F10, which has been cocrystallized with H5 HA and shown to bind

to the F subdomain (*8*) (fig. S7). Using Pepscan analysis, FI6 was tested for binding to overlapping 15-oligomer linear and cyclic peptides of the F subdomain, spanning the C terminus of HA1 and the full HA2 of the H5 A/Vietnam/1194/04 virus, as well as to 26-oligomer homodimeric helical coiled-coil peptides covering the subdomain's A and B helices (*19*). FI6 recognized residues in the fusion peptide (fig. S8A) and helix A of group 1 and group 2 HA subtypes but not helix A of influenza B HA (fig. S8, B and C). Fab fragments were prepared from the optimized FI6v3 antibody and cocrystallized with H1 (group 1) and H3 (group 2) HAs (*20*). Although the two HAs are phylogenetically and structurally distinct and the complexes crystallize with different packing arrangements, the interaction surfaces were found to be similar (fig. S10, A and B) and to agree perfectly with the peptide-binding studies (fig. S8, D and E). In both cases, each monomer of the HA trimer binds one molecule of FI6v3 (Fig. 3). The HCDR3 loop of FI6v3 binds into a shallow groove on the F subdomain of the HAs, where the sides of the groove are formed by residues from helix A of HA2 and parts of two strands of HA1 (38 to 42 and 318 to 320), whereas the bottom is formed by the HA2 turn, encompassing residues 18 to 21 (fig. S10, A and B). The HCDR3 loop crosses helix A, at an angle of about 45 degrees, enabling Leu^{100A}, Tyr^{100C}, Phe^{100D}, and Trp^{100F} to make hydrophobic contacts with residues in the groove (Fig. 4, A and B). Tyr^{100C} and Trp^{100F} also make potential hydrogen bonds with the side chain of Thr^{318} of HA1 and the main-chain carbonyl of residue 19 of HA1, respectively. Two additional polar interactions are formed by main-chain carbonyls at residues 98 and 99 of HCDR3 with Asn^{53} and Thr^{49} on helix A. Taken together, the interaction of HCDR3 with HA (H1 and H3) buries about 750 $Å^2$ of the surface of the antibody, and about two-thirds of this interaction is accounted for by the interaction with the HA2 chain. Overall, the interactions made by FI6v3 with the hydrophobic groove on H1 and H3 are remarkably similar.

The light chain CDR1 (LCDR1) loop of FI6v3 makes two contacts with the side of helix A, opposite the side that contributes to the hydrophobic groove; Phe^{27D} makes hydrophobic contact with the aliphatic part of Lys^{39}, and Asn^{28} hydrogen bonds to Asn^{43}, together accounting for a buried surface area of about 190 $Å^2$ for both H1 and H3. With H1 HA, which was cocrystallized in the uncleaved form, LCDR1 also makes extensive contact with the uncleaved "fusion peptide" of the neighboring HA monomer (Fig. 3, B and C, and Fig. 4, A and B), which accounts for an additional 320 $Å^2$ of FI6v3 buried surface. Residues 28 and 29 of LCDR1 make main-chain amide hydrogen bonds with the main-chain carbonyls of HA1 residue 329 and the next-but-one residue, Leu^2, of HA2 and thus span the cleavage site. Phe^{27D} of LCDR1 makes hydrophobic contacts with Leu^2 of the neighboring HA2, whereas the side-chain hydroxyl of Tyr^{29} hydrogen bonds to the main-chain carbonyl of residue 325 of the neighboring HA1 chain. In contrast to the similar interaction of HCDR3 with H1 and H3 HAs, the interaction of LCDR1 with the fusion peptide from the neighboring cleaved H3 HA monomer is substantially less extensive than the interaction formed with the uncleaved H1 HA (Fig. 3, inset B). Although Phe^{27D}

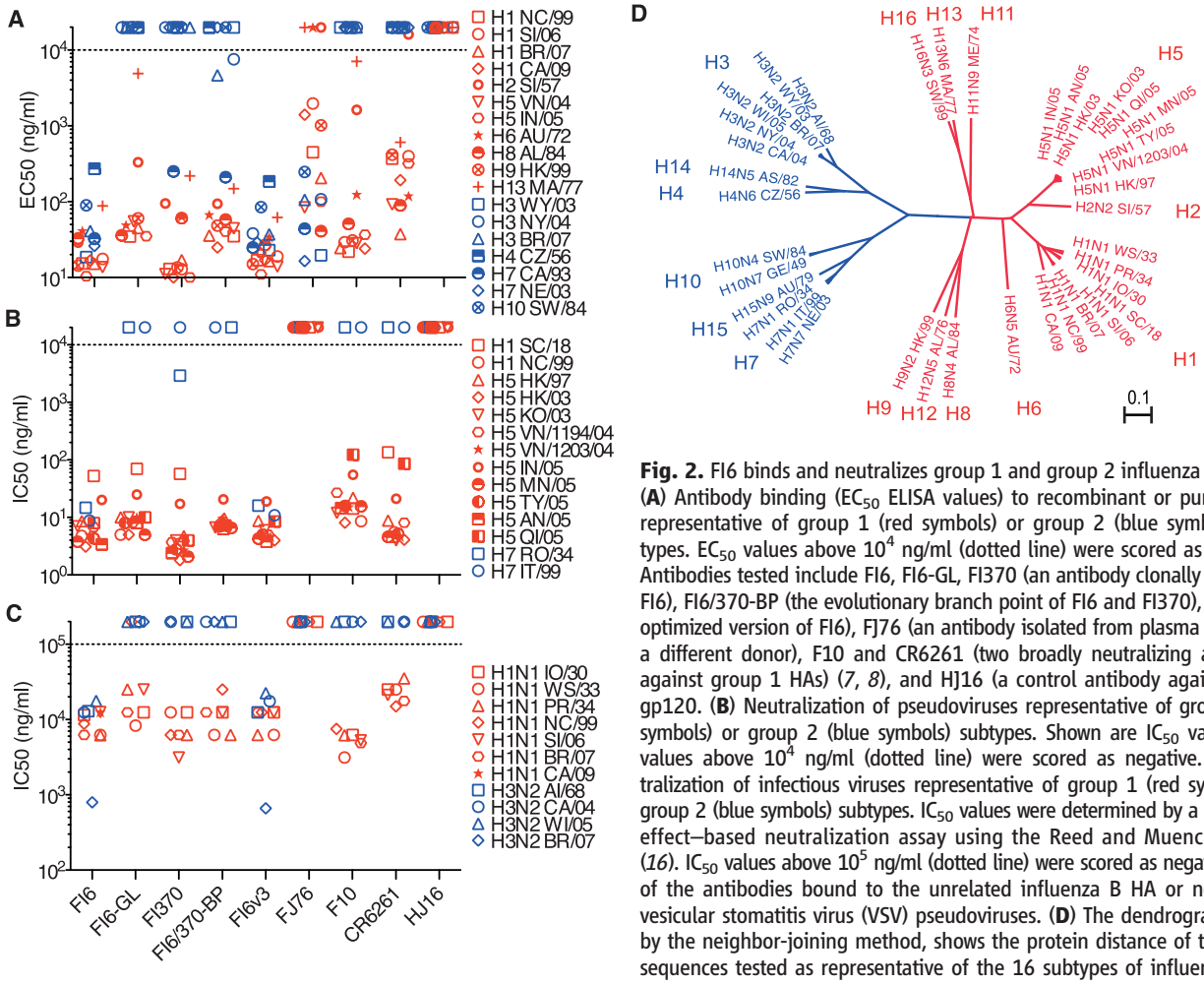

Fig. 2. FI6 binds and neutralizes group 1 and group 2 influenza A viruses. (**A**) Antibody binding (EC_{50} ELISA values) to recombinant or purified HAs representative of group 1 (red symbols) or group 2 (blue symbols) subtypes. EC_{50} values above 10^4 ng/ml (dotted line) were scored as negative. Antibodies tested include FI6, FI6-GL, FI370 (an antibody clonally related to FI6), FI6/370-BP (the evolutionary branch point of FI6 and FI370), FI6v3 (an optimized version of FI6), FJ76 (an antibody isolated from plasma cells from a different donor), F10 and CR6261 (two broadly neutralizing antibodies against group 1 HAs) (*7*, *8*), and HJ16 (a control antibody against HIV-1 gp120. (**B**) Neutralization of pseudoviruses representative of group 1 (red symbols) or group 2 (blue symbols) subtypes. Shown are IC_{50} values. IC_{50} values above 10^4 ng/ml (dotted line) were scored as negative. (**C**) Neutralization of infectious viruses representative of group 1 (red symbols) or group 2 (blue symbols) subtypes. IC_{50} values were determined by a cytopathic effect–based neutralization assay using the Reed and Muench formula (*16*). IC_{50} values above 10^5 ng/ml (dotted line) were scored as negative. None of the antibodies bound to the unrelated influenza B HA or neutralized vesicular stomatitis virus (VSV) pseudoviruses. (**D**) The dendrogram, made by the neighbor-joining method, shows the protein distance of the 39 HA sequences tested as representative of the 16 subtypes of influenza A HA. The amino acid distance scale is indicated with a value of 10% distance. Group 1 subtypes are in red and group 2 subtypes in blue. Complete viral strain designations are listed in (*16*). Experiments were performed in duplicates for binding or in quadruplicates for neutralization assays. Data are representative of at least three independent experiments.

again makes contact with the aliphatic moiety of Lys[39] of HA2, Tyr[29] makes potential hydrogen bond contact with the main-chain carbonyl of Ala[7] of the neighboring HA2 (as opposed to residue 329 in uncleaved H1 HA). In contrast, there are no main-chain contacts between the LCDR1 loop and the fusion peptide of the cleaved H3 HA, which accounts for the smaller contact area of 114 Å^2 (compared with 320 Å^2 in H1 HA). It also seems that cleavage of the HA precursor to produce the H3 HA results in the slightly different orientation of FI6v3 with respect to the HA in the FI6v3-H3 and FI6v3-H1 complexes.

The structures of two cross-reactive antibodies, CR6261 and F10, which are group 1–specific, have previously been reported as complexes with H5 and H1 HAs (Fig. 3, D and E) (*8*, *21*). The binding of CR6261 and F10 antibodies to HA is mediated only by their V_H domains, which are oriented approximately the same as each other with respect to the HA, but both antibodies are significantly rotated relative to FI6v3 and are 5 to 10 Å nearer to the membrane-proximal end of HA (Fig. 3, D and E). The structures of FI6v3-H1 and FI6v3-H3 presented here also reveal that, although the binding sites on HA of the three antibodies overlap extensively, the nature of the interactions made by FI6v3, and presumably FI6, is markedly different from that of those made by CR6261 and F10 antibodies. The most striking difference is that the interaction of FI6v3 with the hydrophobic groove on HA is mediated solely by the long HCDR3, whereas for CR6261 and F10, all three HCDRs are involved in binding (Fig. 4, C and D).

An important difference between the FI6v3-H1 and FI6v3-H3 complexes is that H3 HA is glycosylated at Asn[38] (HA1), as are H7, H10, and H15 HAs of group 2, whereas H1, in common with all group 1 HAs, is not. In the unbound structure of H3 (*22*), this carbohydrate side chain projects from the beta strand of HA1, which contains the Asn[38] residue, toward helix A of HA2 of the same HA subunit, such that it would overlap the footprint of FI6v3 (Fig. 5A). Carbohydrate side chains are known to influence the antigenicity of virus glycoproteins (*23*–*25*); therefore, this overlap has been suggested to account for the lack of binding to group 2 HAs of other group 1 cross-reactive antibodies that target the membrane-proximal region of HA (*8*, *21*).

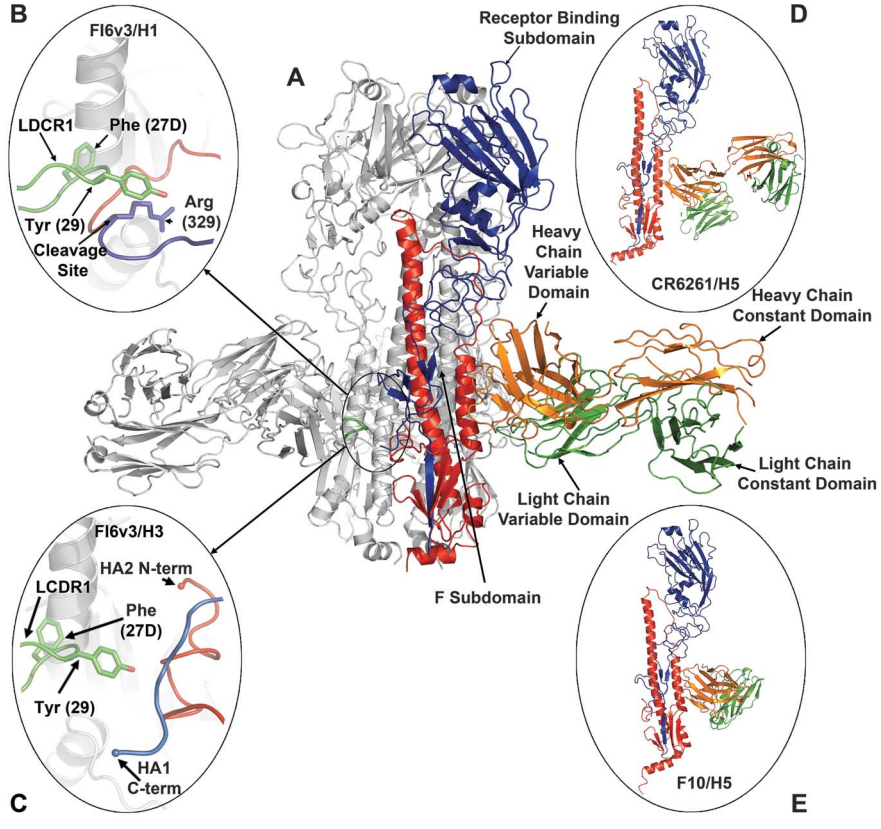

Fig. 3. FI6v3 binding to the F subdomain of the HA trimer. (**A**) Trimer of H3 HA binding three FI6v3 [Protein Data Bank (PDB) identification no. 3ZTJ] antibodies in Ribbons representation. One of the HA monomers is colored blue for HA1 and red for HA2; the other two HA monomers are gray. (**B** and **C**) Enlarged view of the interaction of the LCDR1 loop with the fusion peptide of the neighboring HA in FI6v3-H1 (B) and FI6v3-H3 (C) complexes, respectively. (**D** and **E**) Structures of monomers from H5 HA in complex with CR6261 (PDB 2GBM) (D) and F10 (PDB 3FKU) (E) binding to a region similar to that of FI6v3 but with their V_H domain sitting 5 to 10 Å lower on the HA.

FI6v3 binding to H3 HA, however, is enabled by reorientation of the oligosaccharide, a rotation of about 80° away from the surface of the HA, so that it makes new contacts with Asp[53] and Asn[55] of the HCDR2 loop (Fig. 5B). Given that the flexibility of the carbohydrate side chain at Asn[38] allows it to accommodate FI6v3 binding to H3 HA, we asked whether this glycosylation site was likely to be the reason that H3 HA does not bind to CR6261 or F10. Simple modeling suggests that the same change in orientation of the carbohydrate side chain would be compatible with the binding of the CR6261 (*21*), but not the F10 (*8*), cross-reactive antibodies. The beta turn encompassing V_H residues 73 to 77 of F10 would clash with the Asn[38]-linked carbohydrate in the orientation it adopts in the FI6v3-H3 complex, and it is unclear whether the carbohydrate would be free to rotate further out of the binding site to accommodate F10 binding. However, neither CR6261 nor F10 were able to neutralize an H7 pseudovirus (A/chicken/Italy/99) in which the glycosylation site (Asn[38]) was removed [half maximal inhibitory concentration (IC_{50}) > 50 μg/ml], which indicated that the steric hindrance of the glycan is not the only structural constraint that prevents binding of CR6261 and F10 antibodies to group 2 HAs.

Besides the glycosylation of Asn[38], the most striking difference in the F subdomain structure between group 1 and group 2 HAs involves the group-distinctive environment and orientation of HA2 Trp[21] (*26*, *27*). In group 1 HAs, Trp[21] is approximately parallel to the surface of the F subdomain, whereas in group 2 HAs, it is oriented roughly perpendicular to the surface (Fig. 5, C and D). All three antibodies (FI6v3, CR6261, and F10) make contacts with Trp[21], mainly through a phenylalanine side chain: Phe[100D] on FI6v3, Phe[54] on CR6261, and Phe[55] on F10 (Fig. 5, C and D). In the case of FI6v3, local rearrangements in the HCDR3 loop mean that Phe[100D] sits ~2 Å deeper in the hydrophobic groove in the H1 complex than it does in the H3 complex; it thus maintains a similar contact distance with Trp[21] in both cases. The two group 1–specific antibodies position Phe[54] (CR6261) and Phe[55] (F10) similarly to FI6v3 in complex with H1 HA. However, as Phe[54] (CR6261) and Phe[55] (F10) are located on the short loop of HCDR2, which connects two adjacent antiparallel strands, it seems that there is less flexibility than in FI6v3 for the phenylalanine to move further out of the hydrophobic groove to accommodate the group 2 orientation of Trp[21]. Thus, binding of CR6261 and F10 to group 2 HAs is likely blocked by a steric clash between the HCDR2 phenylalanine and Trp[21]. In summary, the structural data obtained indicate that, although the core epitope on helix A is similar to that recognized by CR6261 and F10, FI6v3 (and likely FI6) binds with a different angle, 5 to 10 Å more membrane distal, and contacts a larger area, embracing helix A and extending to the fusion peptide of the neighboring monomer both in the

cleaved and uncleaved forms (fig. S11). FI6v3 binding is mediated by both V_H and V_K CDRs, with prominent contributions of the long HCDR3, which accommodates different conformations of the group-specific Trp^{21} loop, and of the heavily mutated LCDR1. The use of both V_H and V_K chains and the long HCDR3 are characteristic of naturally selected antibodies and contrast with a property of phage-derived antibodies, such as CR6261 and F10, which bind using only the V_H chain.

Prophylactic and therapeutic efficacy of FI6 and FI6v3 in vivo. The protective efficacy of FI6 and FI6v3 was tested in mice lethally infected with A/Puerto Rico/8/34 (H1N1) virus. In this model, FI6 and FI6v3 showed comparable prophylactic efficacy, as they were fully protective when administered at 4 mg per kg of body weight and partially protective at 2 mg/kg (Fig. 6A and fig. S12). When tested therapeutically at 15 mg/kg in mice lethally infected with A/Puerto Rico/8/34, FI6v3 was able to protect from lethality when administered 1 or 2 days post infection (Fig. 6B). Lung virus titers on day 4 after infection in mice treated with FI6v3 on day 0 or 1 day after infection were reduced to about 1/100th the titers in control antibody-treated mice (fig. S13). FI6v3 was also effective in reducing body weight loss in mice challenged with a H3 HK-x31 reassortant virus, which failed to exert a lethal effect even at the high dose tested (Fig. 6C). Furthermore, FI6 protected ferrets from a lethal challenge with the highly pathogenic H5N1 virus (A/Vietnam/1203/04) (Fig. 6D and fig. S14).

For in vivo experiments aimed at determining the role of antibody effector functions in the protective efficacy of FI6, we produced Fc mutants of FI6 that lacked complement binding (FI6-KA) or complement and Fc receptor (FcR) binding (FI6-LALA) (*28*). These antibodies showed the same binding and in vitro neutralizing properties as FI6 and comparable half-lives in vivo (mean values 3.3, 3.4, and 3.5 days for FI6, FI6-KA, and FI6-LALA, respectively). When administered at 10 mg/kg, FI6 and FI6-KA were fully protective, whereas FI6-LALA showed a substantial loss of activity, as it was able to protect only 40% of the animals (Fig. 6E). This decreased efficacy was particularly evident when mutant antibodies were administered at the limiting concentration of 3 mg/kg (Fig. 6F). These data suggest that in vivo efficacy is substantially dependent on FcR binding, which implies that the killing of infected cells might play a role in limiting infection in vivo. This conclusion is compatible with the finding that FI6 binds effectively to the HA expressed on influenza virus–infected cells (fig. S15).

Mechanisms of neutralization of virus infectivity. From the data obtained, a number of suggestions can be made regarding mechanisms by which FI6 (and the optimized FI6v3 version) might neutralize virus infectivity. The increase in stability of the F subdomain, which would result from high-affinity antibody binding, would be expected to inhibit the conformational changes in HA that are required for membrane fusion (*23*), as shown by the inhibition of syncytia formation (*7*–*9*). Two other mechanisms may be involved in neutralization. In the first, the antibody light chain binding to unprocessed HA0 would block cleavage and hence infectivity, at least for those viruses where cleavage occurs extracellu-

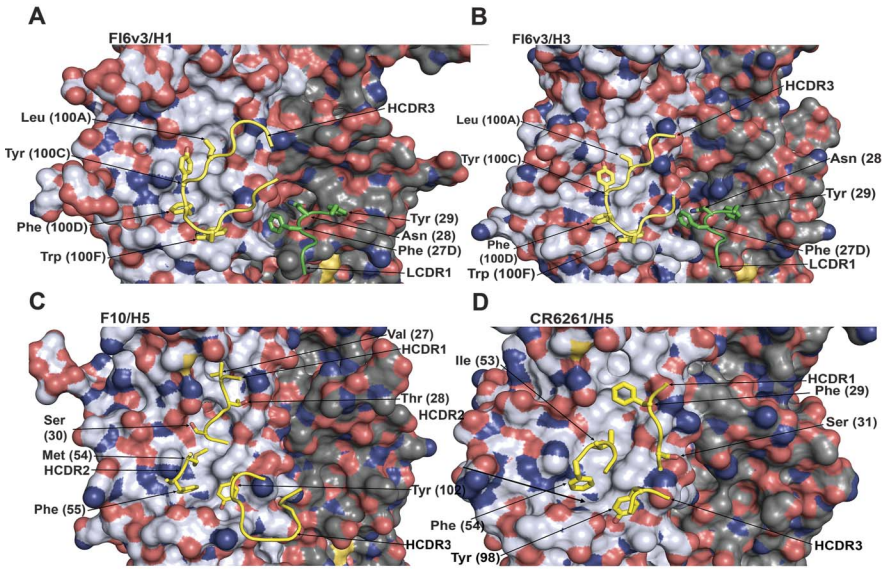

Fig. 4. FI6v3 interactions with the F subdomain of HA. (**A** and **B**) Surface representation of the F subdomain of H1 HA (A) (PDB 3ZTN) and H3 HA (B) colored according to atom type (carbon, gray; oxygen, red; nitrogen, blue; sulfur, yellow) with the HCDR3 and LCDR1 loops of FI6v3 shown as a yellow coil and green coils, respectively, with selected side chains. (**C** and **D**) Similar views of H5 HA in complex with F10 (C) and CR6261 (D) with the HCDR1, HCDR2, and HCDR3 loops as yellow coils.

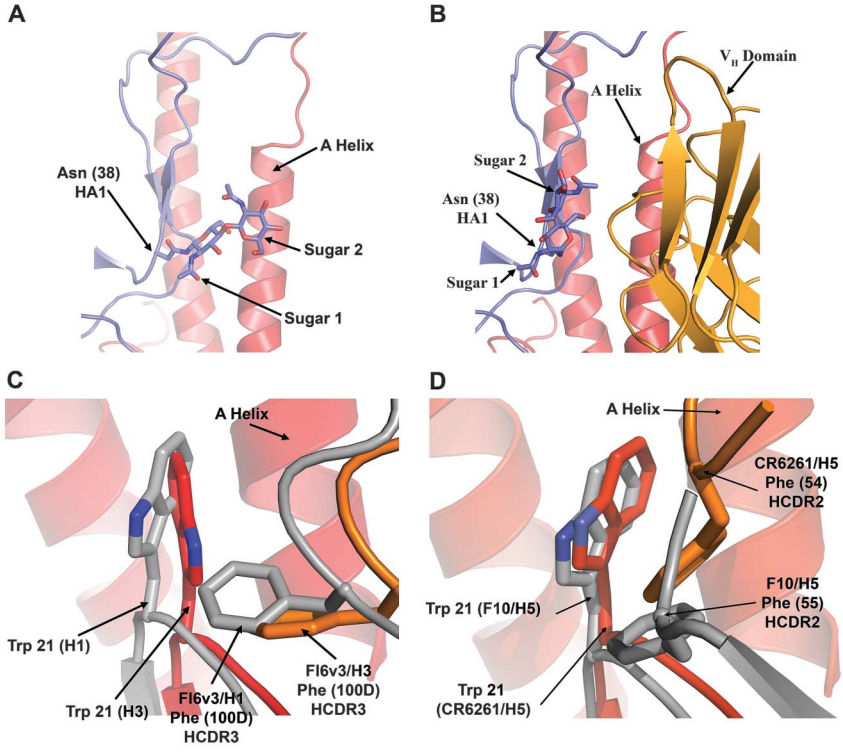

Fig. 5. Group-specific differences at the cross-reactive antibody–binding sites. (**A** and **B**) Positioning of the carbohydrate side chain at Asn^{38} in the H3 HA apo structure (A) and in the FI6v3-bound structure (B). (**C** and **D**) Orientation of HA1 Trp^{21} in different antibody complexes. (C) Phe^{100D} of the HCDR3 loop of FI6v3 interacting with the F subdomain of the HAs. The FI6v3-H3 complex is orange and the FI6v3-H1 complex is gray. (D) The HCDR2 loop of the F10 and CR6261 antibodies presenting Phe^{55} and Phe^{54}, respectively, toward Trp^{21} of H5 HA.

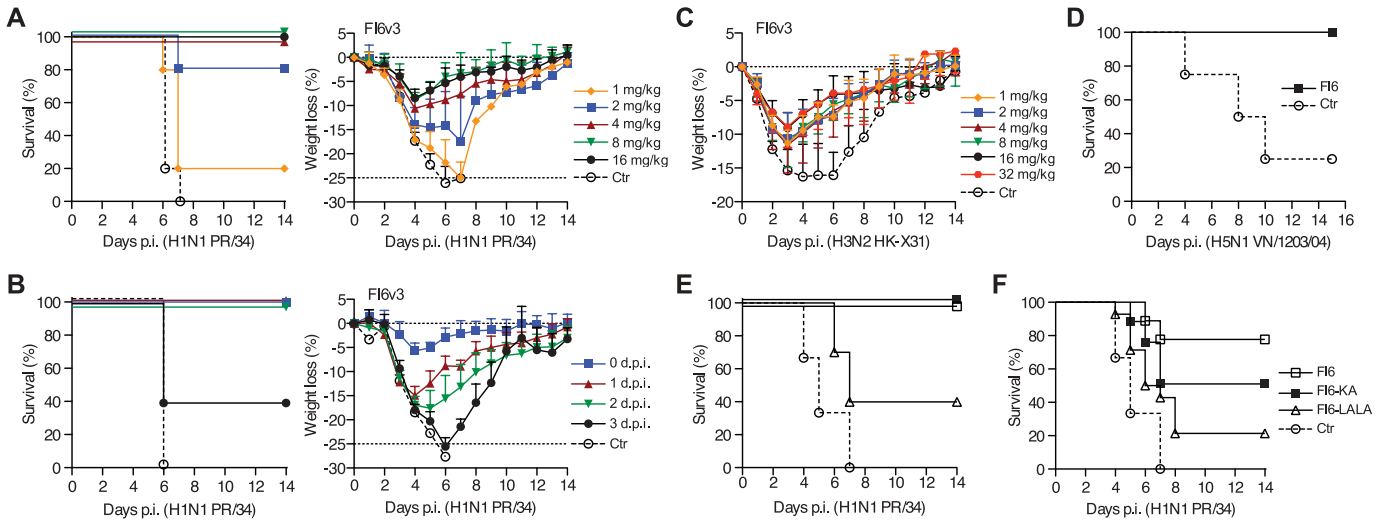

Fig. 6. Passive transfer of FI6 or FI6v3 confers protection to mice and ferrets. Survival curves and body weight loss (**A**) of BALB/c mice (five per experimental condition) that received different doses of FI6v3 or HJ16 as a control intravenously (i.v.) 3 hours before intranasal infection with 10 minimal doses lethal to 50% of mice (MLD_{50}) (2400 median tissue culture infectious doses) of H1N1 PR/34 virus. Shown is one experiment out of three. (**B**) Survival curves and body weight loss of mice (five per experimental condition) that received 15 mg/kg of FI6v3 i.v. on day 0 (3 hours before infection) or on day 1, 2, and 3 after infection with 10 MLD_{50} PR/34 virus. One experiment out of two. (**C**) Body weight loss of mice (10 per experimental condition) that received different doses of FI6v3 i.v. 3 hours before infection with 3×10^5 plaque-forming units (PFUs) H3N2 HK-x31 virus. The reduction of body weight was significant from day 2 to day 8 at the two highest concentrations tested and from day 3 to day 8 at all remaining concentrations tested (*P* values ranging from 0.01 to 0.001 as measured using the two-way analysis of variance method). One experiment out of three. (**D**) Survival curves of ferrets (four per experimental condition) that received 20 mg/kg of FI6 or phosphate-buffered saline as a control 1 day before infection with 10^3 PFUs of H5N1 VN/1203/04. (**E** and **F**) Survival curves of mice (10 per experimental condition) that received 10 mg/kg (E) or 3 mg/kg (F) of FI6, FI6-KA, FI6-LALA, or HJ16 as a control 1 day before infection with PR/34 virus. One experiment out of two. p.i., post infection. Values are means ± SD.

larly (*29*, *30*). This hypothesis is supported by the finding that FI6v3 inhibits cleavage of HA0 by trypsin treated with L-(tosylamido-2-phenyl) ethyl chloromethyl ketone (TPCK trypsin) (fig. S16). In the second, the light-chain interactions with the fusion peptide and the C-terminal HA1 residues of the neighboring subunit may prevent fusion by cross-linking the subunits of the HA trimer (*31*, *32*). In all cases, the efficiency of neutralization would depend on the accessibility to the binding site at the membrane-proximal region of HA (*33*), which is limited by the HA surface coverage on the virus, estimated to vary between 20 and 50% (*34*, *35*). In contrast, on the surface of infected cells, the interaction of FI6 with newly made HA is unlikely to be restricted by spacing considerations, and therefore, the antibody may prevent virus assembly, recruit complement and FcR^+ cytotoxic cells, or act by other mechanisms yet to be defined (*36*).

Concluding remarks. A common objective of studies of antibody-HA complexes is to deduce structural parameters that would direct vaccine design. The importance of helix A in HA-mediated membrane fusion is clear from structural analyses (*37*) and is reflected by the neutralization of virus infectivity by antibodies, such as FI6, CR6261, and F10, or small molecules that target this region (*8*, *21*, *38*). Furthermore, the pan-influenza cross-reactivity of FI6 is also related to its ability to accommodate the group-specific arrangements of residues near Trp^{21}, which are implicated in the activation of membrane fusion at low pH (*26*, *27*). The elicitation of antibodies able to bind helix A and to accommodate the structural differences in the Trp^{21} region represents a favorable characteristic for a pan-influenza vaccine.

The main incentives for our studies of anti-influenza antibodies are the unpredictability of the occurrence of influenza pandemics, the wide range of antigenically novel viruses, and the need for new antiviral treatments of severe influenza infections. The results of prophylaxis and therapy that we report identify FI6 as the first example of a neutralizing monoclonal antibody for potential use against all influenza A viruses.

References and Notes

1. M. Knossow, J. J. Skehel, *Immunology* **119**, 1 (2006).
2. E. Nobusawa *et al.*, *Virology* **182**, 475 (1991).
3. R. G. Webster, W. J. Bean, O. T. Gorman, T. M. Chambers, Y. Kawaoka, *Microbiol. Rev.* **56**, 152 (1992).
4. C. A. Russell *et al.*, *Science* **320**, 340 (2008).
5. S. J. Gamblin, J. J. Skehel, *J. Biol. Chem.* **285**, 28403 (2010).
6. Y. Okuno, Y. Isegawa, F. Sasao, S. Ueda, *J. Virol.* **67**, 2552 (1993).
7. M. Throsby *et al.*, *PLoS ONE* **3**, e3942 (2008).
8. J. Sui *et al.*, *Nat. Struct. Mol. Biol.* **16**, 265 (2009).
9. D. Corti *et al.*, *J. Clin. Invest.* **120**, 1663 (2010).
10. J. Wrammert *et al.*, *J. Exp. Med.* **208**, 181 (2011).
11. T. T. Wang *et al.*, *PLoS Pathog.* **6**, e1000796 (2010).
12. R. Yoshida *et al.*, *PLoS Pathog.* **5**, e1000350 (2009).
13. G. Cassese *et al.*, *J. Immunol.* **171**, 1684 (2003).
14. We observed that IL-6–supplemented medium supports plasma cell survival for at least 4 days. When antibody-secreting cells, as determined by enzyme-linked immunosorbent spot assay (ELISPOT), were seeded at 0.5 cells per well, the amount of antibody produced by single plasma cells was on average 200 to 400 pg per culture, corresponding to an immunoglobulin G (IgG) concentration of 4 to 8 ng/ml in 50 µl. Plating efficiency for IgG-secreting cells ranged from 30 to 80%, as determined by comparison of ELISPOT and enzyme-linked immunosorbent assay (ELISA) data. The sequences of the V_H and the variable region of the immunoglobulin light chain (V_L) gene transcripts were obtained by a modification of the method of Tiller *et al.* (*15*). The efficiency of this process was close to 50%.
15. T. Tiller *et al.*, *J. Immunol. Methods* **329**, 112 (2008).
16. Materials and methods are available as supporting material on *Science* Online.
17. An antibody (called FI6) with the same sequence as FI442, FI510, FI802, and FI804, with the exception of two amino acid substitutions in heavy chain framework region HFR4 and light chain framework region LFR1 (fig. S1), was isolated from a plasma cell of the same donor in December 2008, after seasonal vaccine boost (H1N1 A/Brisbane/59/07, H3N2 A/Brisbane/10/07, and B/Florida/4/06). The two substitutions did not affect binding and neutralization. These findings demonstrate that a clone of memory B cells can repeatedly respond to different influenza HAs without undergoing further somatic mutations.
18. The antibody named FI6v3 utilizes FI6 V_Hv3 and FI6 V_Kv2 variants for heavy and light chains, respectively (fig. S1).
19. J. P. M. Langedijk, M. J. Zekveld, M. Ruiter, D. Corti, J. W. Back, *Anal. Biochem.* **417**, 149 (2011).
20. Because the FI6v3-H1 complex diffracted to better resolution than FI6v3-H3, and produced good-quality electron density maps (fig. S9), the FI6 variable domains were built and refined against the FI6v3-H1 data set after the initial molecular replacement solution and then used for further molecular replacement calculations to solve the FI6v3-H3 complex.
21. D. C. Ekiert *et al.*, *Science* **324**, 246 (2009).
22. S. J. Watowich, J. J. Skehel, D. C. Wiley, *Structure* **2**, 719 (1994).
23. J. J. Skehel, D. C. Wiley, *Annu. Rev. Biochem.* **69**, 531 (2000).
24. M. Sagar, X. Wu, S. Lee, J. Overbaugh, *J. Virol.* **80**, 9586 (2006).

25. J. E. Lee *et al.*, *Nature* **454**, 177 (2008).
26. Y. Ha, D. J. Stevens, J. J. Skehel, D. C. Wiley, *EMBO J.* **21**, 865 (2002).
27. R. J. Russell *et al.*, *Virology* **325**, 287 (2004).
28. A. J. Hessell *et al.*, *Nature* **449**, 101 (2007).
29. E. Böttcher-Friebertshäuser *et al.*, *J. Virol.* **84**, 5605 (2010).
30. W. Garten, H. D. Klenk, *Trends Microbiol.* **7**, 99 (1999).
31. C. Barbey-Martin *et al.*, *Virology* **294**, 70 (2002).
32. L. Godley *et al.*, *Cell* **68**, 635 (1992).
33. D. Fleury *et al.*, *Nat. Struct. Biol.* **6**, 530 (1999).
34. S. Cusack, R. W. Ruigrok, P. C. Krygsman, J. E. Mellema, *J. Mol. Biol.* **186**, 565 (1985).
35. L. J. Calder, S. Wasilewski, J. A. Berriman, P. B. Rosenthal, *Proc. Natl. Acad. Sci. U.S.A.* **107**, 10685 (2010).
36. J. S. Rossman, R. A. Lamb, *Virology* **411**, 229 (2011).
37. P. A. Bullough, F. M. Hughson, J. J. Skehel, D. C. Wiley, *Nature* **371**, 37 (1994).
38. R. J. Russell *et al.*, *Proc. Natl. Acad. Sci. U.S.A.* **105**, 17736 (2008).

Acknowledgments: This work was supported by the European Research Council (grant 250348 IMMUNExplore), the Swiss National Science Foundation (31003A-126027), the Human Frontier Science Program (RGP9/2007), the U.K. Medical Research Council, and the Wellcome Trust. A.L. is supported by the Helmut Horten Foundation. We gratefully acknowledge Diamond for access to synchrotron time. We thank M. Nussenzweig and H. Wardemann for providing reagents for antibody cloning and expression, A. Ritchie at BioFocus for supervising the FI6-H1 structural work, K. Harrod at Lovelace Research Respiratory Institute for supervising the ferret study, E. Soethout at the National Institute for Public Health and the Environment (Netherlands) for providing the H3N2 HK-x31 virus, and W. J. Rutter and L. Varani for critical reading and comments. A.L. is the scientific founder and acting chief scientific officer of Humabs BioMed SA. A.L. and F.S. hold shares in Humabs BioMed SA. The Institute for Research in Biomedicine has two pending patent applications: PCT/IB/2009/007375 (Methods for producing antibodies from plasma cells, A.L. and D.J.) and PCT/US2009/051851 (Neutralizing anti-influenza virus antibodies and uses thereof, A.L.). J.P.M.L. has a patent application on the use of helical peptides for epitope mapping, EP 11160745.3 (Helical peptide libraries for lead identification and interaction site mapping). Antibody sequences for all described FI6 variants are available in fig. S1. Nucleotide sequences for the antibodies described have been deposited in GenBank (accession numbers JN234430, JN234431, JN234432, JN234433, JN234434, JN234435, JN234436, JN234437, JN234438, JN234439, JN234440, JN234441, JN234442, JN234443, JN234444, JN234445, JN234446, JN234447, JN234448). The FI6 and FI6v3 antibodies can be obtained for research purposes under a material transfer agreement.

Supporting Online Material

www.sciencemag.org/cgi/content/full/science.1205669/DC1
Materials and Methods
Figs. S1 to S16
Tables S1 and S2
References (*39*–*46*)

16 March 2011; accepted 1 July 2011
Published online 28 July 2011;
10.1126/science.1205669

REPORTS

Circumstellar Material in Type Ia Supernovae via Sodium Absorption Features

A. Sternberg,[1]* A. Gal-Yam,[1]* J. D. Simon,[2] D. C. Leonard,[3] R. M. Quimby,[4] M. M. Phillips,[5] N. Morrell,[5] I. B. Thompson,[2] I. Ivans,[6] J. L. Marshall,[7] A. V. Filippenko,[8] G. W. Marcy,[8] J. S. Bloom,[8] F. Patat,[9] R. J. Foley,[10] D. Yong,[11] B. E. Penprase,[12] D. J. Beeler,[12] C. Allende Prieto,[13,14] G. S. Stringfellow[15]

Type Ia supernovae are key tools for measuring distances on a cosmic scale. They are generally thought to be the thermonuclear explosion of an accreting white dwarf in a close binary system. The nature of the mass donor is still uncertain. In the single-degenerate model it is a main-sequence star or an evolved star, whereas in the double-degenerate model it is another white dwarf. We show that the velocity structure of absorbing material along the line of sight to 35 type Ia supernovae tends to be blueshifted. These structures are likely signatures of gas outflows from the supernova progenitor systems. Thus, many type Ia supernovae in nearby spiral galaxies may originate in single-degenerate systems.

Type Ia supernovae (SNe Ia) have large and calibratable luminosities, making them good tools for measuring distances on a cosmic scale to gauge the geometry and evolution of the universe (*1*, *2*). Understanding the nature of the progenitor system is important, as progenitor evolution or a changing mix of different progenitors may bias cosmological inferences. The consensus view of SNe Ia is that mass transfer onto a massive carbon-oxygen white-dwarf (WD) star in a close binary leads to a thermonuclear explosion, as the mass of the WD approaches the critical Chandrasekhar mass limit (*3*). In the single-degenerate (SD) model, the mass donor is either a main-sequence star or an evolved subgiant or giant star, whereas in the competing double-degenerate (DD) model it is another WD (*4*).

In the SD scenario, nonaccreted material blown away from the system before the explosion should remain as circumstellar matter (CSM) (*5*); thus, detection of CSM in SN Ia spectra would lend support to the SD model. Patat *et al*. reported such a detection on the basis of time-variable absorption features of the Na I doublet (Na I D_1 and D_2; λ_{D1} = 5896 Å and λ_{D2} = 5890 Å rest-frame wavelengths) in optical spectra of SN 2006X (*6*). These authors suggest that CSM may be common to all SNe Ia, though variation in its detectability can exist due to viewing angle effects. Although multi-epoch high-resolution spectra of SN 2000cx (*7*) and SN 2007af (*8*) exhibited no absorption features or no time variation in them, additional detections were recently reported for three other events: SNe 2007le, 1999cl, and 2006dd (*9*–*11*). Although it has been suggested that Na D absorption could not have been caused by CSM owing to ionization considerations (*12*), detailed arguments to the contrary have been presented (*9*, *13*).

Absorption features from unrelated intervening gas clouds are expected to have random velocity offsets with respect to the SN, whereas absorption due to winds blown by the progenitor system is expected to be always blueshifted with respect to the SN, because the source of light is behind the outflowing absorbing material. We thus searched for this signature in a large sample of high-resolution, single-epoch observations of SNe Ia. Our sample consisted of spectra of 35 SNe Ia and 11 core-collapse (CC) SNe obtained with the Keck HIRES and Magellan MIKE spectrometers. We also studied previously published spectra of six SNe Ia (*6*, *14*–*17*) and seven CC SNe (*16*–*22*). A bias may exist if other spectra were obtained but not published. Therefore, we report results separately with and without these historical SNe (hereafter "the extended sample," for which results are given in square brackets). Detailed analyses of a few events from our

[1]Benoziyo Center for Astrophysics, Faculty of Physics, Weizmann Institute of Science, Rehovot 76100, Israel. [2]Observatories of the Carnegie Institution of Washington, 813 Santa Barbara Street, Pasadena, CA 91101, USA. [3]Department of Astronomy, San Diego State University, San Diego, CA 92182, USA. [4]Cahill Center for Astrophysics, California Institute of Technology, Pasadena, CA 91125, USA. [5]Carnegie Observatories, Las Campanas Observatory, Casilla 601, La Serena, Chile. [6]Department of Physics and Astronomy, The University of Utah, Salt Lake City, UT 84112, USA. [7]Department of Physics, Texas A&M University, 4242 TAMU, College Station, TX 77843, USA. [8]Department of Astronomy, University of California, Berkeley, CA 94720–3411, USA. [9]European Southern Observatory (ESO), Karl Schwarzschild Strasse 2, 85748, Garching bei München, Germany. [10]Clay Fellow, Harvard-Smithsonian Center for Astrophysics, 60 Garden Street, Cambridge, MA 02138, USA. [11]Research School of Astronomy and Astrophysics, The Australian National University, Mount Stromlo Observatory, Cotter Road, Weston ACT 2611, Australia. [12]Department of Physics and Astronomy, Pomona College, 610 North College Avenue, Claremont, CA 91711, USA. [13]Instituto de Astrofísica de Canarias, 38205, La Laguna, Tenerife, Spain. [14]Departamento de Astrofísica, Universidad de La Laguna, 38206, La Laguna, Tenerife, Spain. [15]Center for Astrophysics and Space Astronomy, University of Colorado, 389-UCB, Boulder, CO 80309, USA.

*To whom correspondence should be addressed. E-mail: assaf.sternberg@weizmann.ac.il (A.S.), avishay.gal-yam@weizmann.ac.il (A.G.)